Eur. Phys. J. B **76**, 481–486 (2010)
DOI: 10.1140/epjb/e2010-00238-7

THE EUROPEAN PHYSICAL JOURNAL B

Regular Article

Hydrogen adsorption on graphene: a first principles study

V.V. Ivanovskaya[1,2,a], A. Zobelli[3], D. Teillet-Billy[1], N. Rougeau[1], V. Sidis[1], and P.R. Briddon[4]

[1] Institut des Sciences Moléculaires d'Orsay, Université Paris-Sud, CNRS, 91405 Orsay, France
[2] Institute of Solid State Chemistry, Ural division of Russian Academy of Science, 620041, Ekaterinburg, Russia
[3] Laboratoire de Physique des Solides, Université Paris-Sud, CNRS UMR 8502, 91405, Orsay, France
[4] Department of Physics, University of Newcastle upon Tyne, Newcastle NE1 7RU, United Kingdom

Received 2 April 2010/ Received in final form 14 June 2010
Published online 3 August 2010 –

Abstract. We present a systematic ab initio study of atomic hydrogen adsorption on graphene. The characteristics of the adsorption process are discussed in relation with the hydrogenation coverage. For systems with high coverage, the resultant strain due to substrate relaxation strongly affects H atom chemisorption. This leads to local structural changes that have not been pointed out to date, namely localized surface curvature. We demonstrate that the hydrogen chemisorption energy barrier is independent of the optimization technique and system size, being associated with the relaxation and rehybridization of the sole adsorbent carbon atom. On the other hand, the H desorption barrier is very sensitive to a correct structural relaxation and is also dependent on the degree of system hydrogenation.

1 Introduction

The interaction of hydrogen with graphitic materials is a field of great current interest owing to its involvement in several areas of fundamental science and technology, namely hydrogen storage in carbon-based systems [1–4], functionalization of graphene by H-doping [5,6], hydrogen erosion of graphite tiles of fusion reactors [7–10] and molecular hydrogen formation on carbonaceous dust grains in the interstellar medium [11–15]. In this context, the adsorption of a single H atom on graphitic like surfaces, i.e. graphite, graphene or polycyclic aromatic hydrocarbons, has been well studied both at the experimental [5,6,16–18] and theoretical levels [19–25].

Experimentally, it has long been considered that, aside from physisorption at very low temperature (<30 K), H atoms do not stick onto a clean defect free graphite surface [26]. However, in accordance with theoretical predictions [19,27–29], Zecho et al. showed experimentally [30,31] that, contrary to earlier belief, H(D) atoms do stick onto the (0001) graphite surface when emitted from a 2000 K thermal source, that is with a maxwellian most probable energy of 0.2 eV. Likewise, all experiments to date use a hot (1600 K–2200 K) H atom beam source to chemisorb H atoms onto graphite or graphene [32–37]. Very recently, the synthesis of highly hydrogenated graphene has also been reported [5,38,39] thereby lending support to an earlier prediction of the existence of graphane [40]. Interestingly, reversible hydrogenation of graphene has been observed which may result in different hydrogen coverage and lead to variable lattice spacing and tunable electronic properties [5,38].

First principles electronic structure calculations based on density functional theory (DFT) on H chemisorption on graphitic like structures were conducted using both cluster [19,20,27] and periodic [28,29,41–43] approaches. In general, it has been shown that chemisorption occurs solely on top of a C atom, which protrudes outside of the flat graphene plane changing its hybridization into a mixed sp^2-sp^3 state. In the [H + graphene] configuration space the path connecting the free hydrogen atom to the chemisorbed one passes through a metastable state corresponding to physisorption onto the flat undistorted surface. Physisorbed and chemisorbed states are thus separated by an energy barrier, which explains why H chemisorption does not spontaneously occur at low temperatures. While this description of the adsorption process is generally accepted, one notices that the characteristic equilibrium atom positions and binding energies reported by different authors exhibit a large dispersion. Binding energies, for instance, lie between 0.47 eV [27] and 1.44 eV [44] or even 1.9 eV [45], with a majority of data between 0.6 eV and 0.85 eV.

This variability can be ascribed to differences in structures, optimization strategies and computational methodology used for modeling H chemisorption on graphite. Uncertainties of the order of few tenths of an eV on the adsorption energy might be critical when one is interested in processes occurring at low temperatures, such as H_2 catalytic formation in the interstellar medium. Moreover, when considering high hydrogen coverage of graphene it is critical to correctly model even the smallest

[a] e-mail: viktoria.ivanovskaya@u-psud.fr

structural perturbations caused to the substrate. It is thus desirable to investigate in a systematic and consistent way how structural relaxation effects manifest themselves and eventually add up. Thus, we survey earlier studies in relation with new methodical calculations and we discuss effects arising from the variation of hydrogenation coverage and extent of system relaxation. Finally, this study sheds new light on H chemisorption onto graphene by drawing attention to some structural and energetic features that have not been discussed before.

2 Computational details

We performed electronic structure calculations and structural optimizations within the framework of DFT using the Perdew-Burke-Ernzerhof (PBE) [46] gradient corrected generalized gradient approximation (GGA) functional for exchange and correlation as implemented in the AIMPRO code [47,48]. Carbon and hydrogen pseudopotentials are generated using the Hartwingsen-Goedecker-Hutter scheme [49]. Valence orbitals are represented by a set of cartesian- gaussians of *s*-, *p*-, and *d*-type basis functions centered at the atomic sites. For hydrogen and carbon, we use large basis sets of 24 and 22 independent functions, respectively. These are based on gaussians of six (*pppppp*, for H) and four (*pdpp*, for C) different exponents multiplied by the standard cartesian prefactors. For the hydrogen basis these gaussians are multiplied by prefactors giving *s*- and *p*-type functions (four functions in total for each exponent); for the carbon basis the gaussians of second-smallest exponent is multiplied by cartesian prefactors to give *s*-, *p*-,and *d*-type functions (10 functions in total), the other exponents are multiplied by cartesian prefactors to give *s*- and *p*-type functions.

We first tested the chosen basis set against known properties of the studied systems. Our cohesion energy (E_{coh}) for the H_2 molecule is 4.53 eV, in good agreement with a previous theoretical value of 4.56 eV [28] and experimental value of 4.75 eV [50]. E_{coh} for graphene is found to be 7.73 eV/atom, compared to the range of theoretical values of 7.2–7.6 [51] and 7.9 eV/atom [52] and to the experimental value for graphite of 7.43 eV/atom [53][1]. We obtain an equilibrium lattice parameter for graphene of 2.475 Å which is in good agreement with the experimental values of 2.456 Å for graphite [55] and 2.46 ± 0.02 Å for graphene [5].

In order to simulate different coverages, calculations on the interaction of atomic hydrogen with graphene have been carried out for a series of $n \times n \times 1$ supercells (n = 2–8). Atomic positions have been optimized using a conjugate gradient scheme until the forces are less than 10^{-4} eV/Å. Electronic structure convergence is ensured by constraining the energy difference in the self-consistent cycle to be below 10^{-8} eV[2]. For each supercell size, energy convergence has been obtained using k-points generated from a Monkhorst-Pack set sampling of the Brillouin zone. The out of plane cell parameter is 20 Å, avoiding inter-plane interactions. Spin polarization has been taken explicitly into account.

In order to compare relative structural stabilities, formation energies (E_{form}) have been determined as:

$$E_{form} = E(H + C_x) - (x\mu_C + E(H)) \quad (1)$$

where E_{H+C_x} is the total internal energy of a system of x carbon atoms with one chemisorbed hydrogen, μ_C is the chemical potential for carbon calculated with respect to graphene (this is a function of the unit cell parameters chosen) and (E_H) is the total energy of the free H atom.

We have considered the effect on E_{form} values of the basis set superposition error (BSSE) due to the use of a localized basis set in the calculations, using the counterpoise method [56]. We find that for our basis set the influence of BSSE is negligable, increasing E_{form} by at most 0.02 eV.

To study the reaction path for H atom adsorption onto graphene and to determine the corresponding activation energy barrier, the nudged elastic band method (NEB) has been employed. The method has been proven to be an efficient technique to explore a large region of configuration space [57–59]. In order to correctly describe the reaction path, we have used a high number of intermediate images, typically 25, allowing all atoms to move within the NEB optimization process.

3 Results and discussion

3.1 Graphene relaxation upon H atom adsorption

The importance of structural relaxation upon hydrogen chemisorption was first noted by Sidis et al. [19,27] and Sha and Jackson [28,29] who showed that chemisorption can only occur when the substrate is allowed to relax. This is due to simultaneous rehybridization of the valence orbitals of the H-bonded C atom, resulting in a local partial loss of aromaticity. However, those early studies only optimised the carbon atom directly attached to the H atom. Later, contradictory statements have appeared in the literature concerning the importance of relaxation of the surrounding carbon atoms: in some works this relaxation was claimed to be negligible [29,41,42] whereas it was asserted to be quite substantial in others [21,44,60]. Moreover, contradictory statements have recently appeared on the H chemisorption formation energy dependence [21] or independence [61] upon the supercell size.

[1] The cohesion energy of graphite should differ from that of graphene by the interlayer van der Waals interactions not reproduced by DFT GGA calculations; from experiments the interlayer cohesion energy is found to be only 0.04 eV/atom [54].

[2] Stringent convergence criteria for both energies and forces are needed since for large supercells during optimization the system lies in a nearly flat energy region of the configuration space. Less strict convergence criteria lead to a non equilibrium configuration and to an overestimation of the formation energy of the order of 0.1 eV.

Table 1. Equilibrium height of the adsorbent carbon atom above the surface (h, Å) and formation energies (E_{form}, eV) for different cell sizes and hydrogen coverage (Θ, %). n is the number of carbon atoms allowed to co-relax with the H atom: the sole adsorbent C (ads. C), all atoms up to the third neighbor (3rd neigh.), all atoms within the cell (all), all atoms simultaneously with cell parameters optimization (all+cell opt). For the comparison with previous works all present results other than "all + cell opt." were obtained with the unit cell parameter fixed at the experimental value of 2.46 Å.

Cell	Θ	n	h this work	h literature	E_{form} this work	E_{form} literature
(2×2)	12.5	ads. C	0.36	0.36 [28]	−0.69	−0.67 [28]
		all	0.36	0.36 [21]	−0.77	−0.75 [21]; −0.83 [61]
		all+cell opt.	0.35		−0.85	
(3×3)	5.6	all+cell opt.	0.51		−0.84	
(4×4)	3.1	ads. C	0.36		−0.67	
		3rd neigh.	0.54		−0.85	
		all	0.58	0.48 [21]; 0.49 [22]	−0.87	−0.79 [21]; −0.89 [22]; −0.85 [23]; −0.76 [24]
		all+cell opt.	0.58		−0.89	
(5×5)	2.0	all+cell opt.	0.63		−0.94	
(6×6)	1.4	all+cell opt.	0.66		−0.96	
(7×7)	1.0	all+cell opt.	0.64		−0.97	
(8×8)	0.8	ads. C	0.35		−0.83	
		3rd neigh.	0.52		−0.96	
		all	0.57		−0.97	−0.87 [63]
		all+ cell opt.	0.57		−0.97	

Therefore, here we consider the H adsorption effects for different system sizes and extent of system optimization. A $(n \times n)$ cell corresponds to a $0.5 \cdot n^{-2}$ coverage. Thus small cell sizes model a regular high hydrogen coverage of a graphene plane, entailing non-negligible hydrogen-hydrogen interactions. Zhou et al. [62] have recently shown that regularly highly hydrogenated graphene presents a ferromagnetic magnetic order. It is thus justified to take into account only one H atom per unit cell for modeling different coverages.

Sha et al. [28,29,41] claimed that the structural relaxation of the C atoms near the chemisorption site is negligible in a (2×2) cell and thus went on fixing all carbon atoms except the adsorbent C atom in their calculations. However as shown in Table 1, the optimization of H and the sole C adsorbent atom leads to a significant underestimation (∼0.1–0.2 eV) of the formation energies even if the equilibrium height of the adsorbent C atom (0.36 Å) is independent of the number of optimized atoms in the system.

We next simultaneously optimize atomic positions and cell parameters for a series of supercells (Tab. 1). For all cell sizes we find the bond lengths between the bonding carbon and its first neighbours to be stretched to 1.50 Å compared to the bond length in graphene (1.42 Å), approaching the diamond bond length of 1.54 Å. The other bond lengths are practically unaffected, and the C-H distance is always found to be 1.13 Å.

For small cells this increase of the C-C bond lengths close to the adsorbent site results in a slight cell parameter increase, e.g. 0.62% for a (2×2) cell. We note that this C-C bond elongation related to the rehybridization at the adsorbent site is also responsible for the lattice parameter expansion found in graphane [64,65]. On the whole, for small systems we find that simultaneous atomic position and cell parameter optimization lead to a significant lowering (of about 0.1 eV) of the formation energies as compared with fully optimized systems with fixed cell parameter, see Table 1. With the enlargement of the supercell size this energy lowering weakens progressively and the cell parameter increase becomes insignificant.

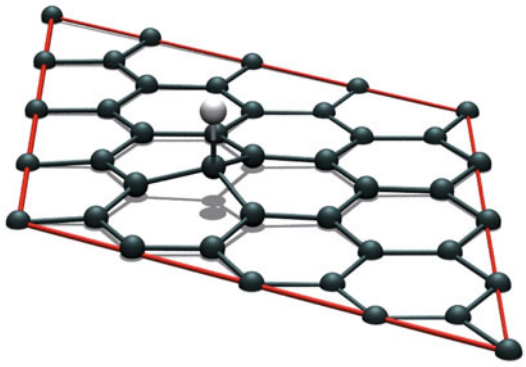

Fig. 1. (Color online) Local distortions around adsorbent C atom at H chemisorption at full (4×4) cell relaxation. Atoms with an out of plane displacement upon H atom chemisorption produce shadows on the substrate plane.

For lower hydrogenation coverages, i.e. larger cells, we find that the vertical displacement of the adsorbent C atom is about 0.5–0.7 Å, accompanied by an upward movement up to a maximum of 0.2–0.3 Å for first neighbor

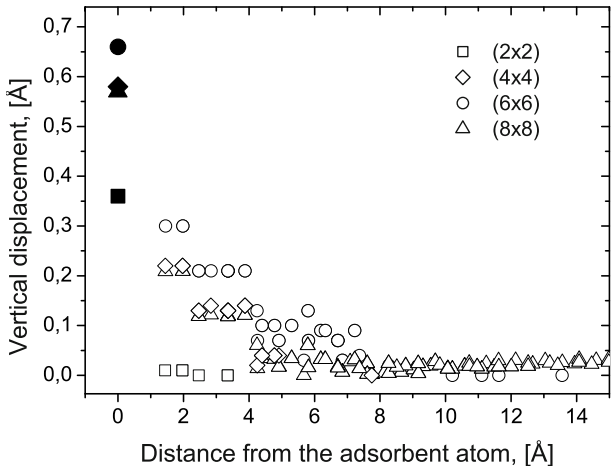

Fig. 2. Vertical displacements of atoms versus in-plane distance from the adsorbent carbon atom. Squares, diamonds, circles and triangles stand for (2×2), (4×4), (6×6) and (8×8) supercells, respectively. The position of the adsorbent atom for each supercell is marked by a closed symbol.

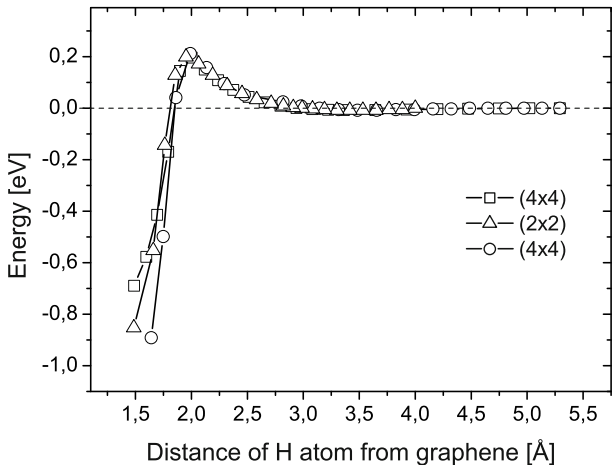

Fig. 3. Comparison of energy curves for adsorption of an H atom onto graphene: squares, optimization of the sole adsorbent C atom within a (4×4) cell; triangles and circles, full NEB relaxation of (2×2) and (4×4) cells, respectively.

and 0.1 Å for second and third neighbor atoms. This behavior results in a local hillock within the graphene layer, see Figure 1. It is interesting that despite this surface curvature, a formation energy accuracy as good as 0.02 eV is achieved when relaxation is restricted to just up to the third nearest neighbors (Tab. 1).

This extended puckering reaches a maximum in the (6×6) supercell, see Figure 2, while for the largest cells considered the hillock height slightly decreases. We conclude that a high hydrogen coverage (inherent to small cells) leads both to a general corrugation of the graphene plane and to slight changes in the unit cell parameter. The strong structural changes in small cells are due to high strain energies and electronic H-H interactions between adjacent cells. For large cells the H induced strain can distribute in plane over a large number of carbon atoms surrounding the chemisorption site and thus the vertical displacement is lower.

3.2 Energy barriers upon hydrogen adsorption and desorption

Since the work of reference [19] the barrier associated with H atom pinning on a graphitic surface has been repeatedly investigated [23,28,41,60,61,66,67]. In Section 3.1 we have shown how the supercell choice and optimization approach may affect the structural and energetic characteristics of the system. Therefore, here we recalculate the energy barriers within the NEB formalism for a series of $(n \times n$, $n = 2$, 4 and 6) supercells allowing free motions of all atoms in the cell. As end points of the reaction path, we use the atomic and cell optimized structures for the H atom bound to graphene and the H atom located 5 Å above the graphitic plane.

Figure 3 shows interaction energies as a function of the hydrogen distance from the graphene plane. We obtain energy barriers for H adsorption of 0.20, 0.21 and 0.22 eV for the (2×2), (4×4) and (6×6) cells, respectively. These values are comparable with barriers of about 0.20 eV and 0.25 eV obtained in recent NEB calculation on (5×5) [67] and (6×6) [61] cells, respectively. For comparison we also present the energy curve obtained when only one carbon atom beneath H is allowed to relax. In this case, in accord with previous calculations we find a barrier of 0.20 eV. In agreement with previous works [27,28] we find a physisorption well of 8 meV at about 3 Å. This value is known to be underestimated by the usage of GGA functionals. To our knowledge the best ab initio determination of the discussed physisorption charactersitics were obtained from MP2 calculations on the H-coronene system [68] which gives a physisorption energy of about 40 meV at an H distance from the plane of 3.1 Å.

Thus we conclude that the main contribution to the chemisorption barrier comes from the relaxation and rehybridisation of the adsorbent carbon atom directly beneath the H atom; the number of optimized atoms and supercell size play a minor role for the determination of the barrier. On the other hand the H atom desorption barrier is quite sensitive to these parameters. From Table 1 and Figure 3 it can be seen that the desorption energy may vary as much as 0.22 eV depending on the hydrogenation coverage or degree of optimization.

4 Conclusions

In this paper we have presented a systematic study of atomic hydrogen adsorption onto graphene, demonstrating the sensitivity of the formation energy and structural characteristics upon the hydrogenation coverage. In contrast with conclusions drawn recently in reference [61] we clearly show that the H-graphene chemisorption characteristics depend strongly upon the supercell size.

We have considered simultaneous relaxation of atom positions and cell parameters for different supercell sizes.

We find a slight relaxation of the cell parameter, which decreases the formation energy by about 0.1 eV for the smallest cell. This energy decrease gradually reduces with the enlargement of the supercell size. We find that the formation energy converges to a value of −0.97 eV for hydrogen coverages less than 2%. H atom chemisorption induces the formation of a hillock around the adsorption spot, in addition to the well established upward movement of the adsorbent C atom. This effect is related to high strain energies and H-H interactions between adjacent cells; in the limit of single hydrogen atom adsorption the hillock height slightly reduces.

Finally, taking into account the structural perturbations, we revisited the estimation of hydrogen chemisorption energy barriers by means of DFT NEB calculations. We find that the H adsorption barrier does not depend on the degree of relaxation or on the cell dimension being associated solely with the movement of the adsorbent carbon atom. Nevertheless, the H desorption barrier is quite sensitive to a correct description of the structure and to the supercell size, i.e. to the hydrogen coverage. In the limit of a single hydrogen atom interacting with graphene, besides the well established chemisorption barrier of 0.2 eV, the desorption barrier corresponds to 1.17 eV.

V.V.I. and A.Z. thank C.P. Ewels and J P. Goss for interesting and helpful discussions. The authors acknowledge support from the Agence Nationale de la Recherche (ANR) in the framework of the IRHONI No. ANR-07-BLAN-0129-2 contract.

References

1. S. Patchkovskii, J. Tse, S. Yurchenko, L. Zhechkov, T. Heine, G. Seifert, PNAS **102**, 10439 (2005)
2. M. Nijkamp, J. Raaymakers, A. van Dillen, K. de Jong, Appl. Phys. Lett. **72**, 619 (2001)
3. A. Zuttel, C. Nutzenadel, P. Sudan, P. Mauron, C. Emmenegger, S. Rentsch, L. Schlapbach, A. Weidenkaff, T. Kiyobayashi, J. Alloys Compd. **330**, 676 (2002)
4. C. Ahn, Y. Ye, B. Ratnakumar, C. Witham, R. Bowman, B. Fultz, Appl. Phys. Lett. **73**, 3378 (1998)
5. D.C. Elias, R. Nair, T. Mohiuddin, S. Morozov, P. Blake, M. Halsall, A. Ferrari, D. Boukhvalov, M. Katsnelson, A. Geim et al., Science **323**, 610 (2009)
6. S. Ryu, M.Y. Han, J. Maultzsch, T.F. Heinz, P. Kim, M.L. Steigerwald, L.E. Brus, Nano Lett. **8**, 4597 (2008)
7. G. Federici, C. Skinner, J. Brooks, J. Coad, C. Grisolia, A. Haasz, A. Hassanein, V. Philipps, C. Pitcher, J. Roth et al., Nucl. Fusion **41**, 1967 (2001)
8. M. Mayer, V. Philipps, P. Wienhold, H. Esser, J. von Seggern, M. Rubel, J. Nucl. Mater. **290**, 381 (2001)
9. Y. Hirohata, Y. Oya, H. Yoshida, Y. Morimoto, T. Arai, K. Kizu, J. Yagyu, K. Masaki, Y. Gotoh, K. Okuno et al., J. Nucl. Mater. **329**, 785 (2004)
10. K. Masaki, K. Sugiyama, T. Hayashi, K. Ochiai, Y. Gotoh, T. Shibahara, Y. Hirohata, Y. Oya, N. Miya, T. Tanabe, J. Nucl. Mater. **337**, 553 (2005)
11. V. Pirronello, C. Liu, J. Roser, G. Vidali, Astron. Astrophys. **344**, 681 (1999)
12. W. Duley, Mon. Not. R. Astron. Soc. **279**, 591 (1996)
13. S. Gough, C. Schermann, F. Pichou, M. Landau, I. Cadez, R. Hall, Astron. Astrophys. **305**, 687 (1996)
14. M. Cacciatore, M. Rutigliano, Plasma Sour. Sci. Technol. **18** (2009)
15. G. Pascoli, A. Polleux, Astron. Astrophys. **359**, 799 (2000)
16. P. Ruffieux, O. Gröning, P. Schwaller, L. Schlapbach, P. Gröning, Phys. Rev. Lett. **84**, 4910 (2000)
17. N.P. Guisinger, G.M. Rutter, J.N. Crain, P.N. First, J.A. Stroscio, Nano Lett. **9**, 1562 (2009)
18. A. Nikitin, L.A. Naeslund, Z. Zhang, A. Nilsson, Surf. Sci. **602**, 2575 (2008)
19. L. Jeloaica, V. Sidis, Chem. Phys. Lett. **300**, 157 (1999)
20. Y. Ferro, F. Marinelli, A. Allouche, J. Chem. Phys. **116**, 8124 (2002)
21. S. Casolo, O.M. Lovvik, R. Martinazzo, G.F. Tantardini, J. Chem. Phys. **130**, 054704 (2009)
22. P.A. Denis, F. Iribarne, J. Mol. Struct, Theochem **907**, 93 (2009)
23. L. Hornekaer, E. Rauls, W. Xu, Z. Šljivancanin, R. Otero, I. Stensgaard, E. Laegsgaard, B. Hammer, F. Besenbacher, Phys. Rev. Lett. **97**, 186102 (2006)
24. E.J. Duplock, M. Scheffler, P.J.D. Lindan, Phys. Rev. Lett. **92**, 225502 (2004)
25. S.F.J. Cox, S.P. Cottrell, M. Charlton, P.A. Donnelly, C. Ewels, M. Heggie, B. Hourahine, J. Phys. Condens. Matter **13**, 2169 (2001)
26. G. Vidali, J. Roser, G. Manico, V. Pirronello, H. Perets, O. Biham, J. Phys. Conf. Ser. **6**, 36 (2005)
27. V. Sidis, L. Jeloaica, A. Borisov, S.A. Deutscher, *Molecular hydrogen in space*, edited by F. Combes, G. Pineau des Forêts, Cambridge Contemporary Astrophysics series (Cambridge University Press, 2000)
28. X. Sha, B. Jackson, Surf. Sci. **496**, 318 (2002)
29. X. Sha, B. Jackson, D. Lemoine, J. Chem. Phys. **116**, 7158 (2002)
30. T. Zecho, A. Guttler, X. Sha, B. Jackson, J. Kuppers, J. Chem. Phys. **117**, 8486 (2002)
31. T. Zecho, A. Güttler, X. Sha, D. Lemoine, B. Jackson, J. Küppers, Chem. Phys. Lett. **366**, 188 (2002)
32. T. Zecho, A. Güttler, J. Küppers, Carbon **42**, 609 (2004)
33. A. Andree, M. Lay, T. Zecho, J. Küpper, Chem. Phys. Lett. **425**, 99 (2006)
34. A. Allouche, Y. Ferro, T. Angot, C. Thomas, J. Layet, J. Chem. Phys. **123**, 124701 (2005)
35. R. Balog, B. Jørgensen, J. Wells, E. Lægsgaard, P. Hofmann, F. Besenbacher, L. Hornekær, J. Am. Chem. Soc. **131**, 8744 (2009)
36. S. Baouche, G. Gamborg, V. Petrunin, A. Luntz, A. Baurichter, L. Hornekær, J. Chem. Phys. **125**, 084712 (2006)
37. C. Thomas, T. Angot, J. Layet, Surf. Sci. **602**, 2311 (2008)
38. P. Sessi, J.R. Guest, M. Bode, N.P. Guisinger, Nano Lett. **9**, 4343 (2009)
39. Z. Luo, T. Yu, K.-j. Kim, Z. Ni, Y. You, S. Lim, Z. Shen, S. Wang, J. Lin, ACS Nano **3**, 1781 (2009)
40. J.O. Sofo, A.S. Chaudhari, G.D. Barber, Phys. Rev. B **75**, 153401 (2007)
41. X. Sha, B. Jackson, D. Lemoine, B. Lepetit, J. Chem. Phys. **122**, 014709 (2005)
42. X. Sha, B. Jackson, J. Am. Chem. Soc. **126**, 13095 (2004)
43. Y. Ferro, F. Marinelli, A. Allouche, Chem. Phys. Lett. **368**, 609 (2003)

44. D.W. Boukhvalov, M.I. Katsnelson, A.I. Lichtenstein, Phys. Rev. B **77**, 035427 (2008)
45. S. Letardi, M. Celino, F. Cleri, V. Rosato, Surf. Sci. **496**, 33 (2002)
46. J.P. Perdew, K. Burke, M. Ernzerhof, Phys. Rev. Lett. **77**, 3865 (1996)
47. R. Jones, P. Briddon, Semicond. Semimetals **51A**, 287 (1998)
48. M. Rayson, P. Briddon, Comput. Phys. Commun. **178**, 128 (2008)
49. C. Hartwigsen, S. Goedecker, J. Hutter, Phys. Rev. B **58**, 3641 (1998)
50. K. Huber, G. Herzberg, *Molecular structure and molecular spectra IV: constants of diatomic molecules* (Van Rostrand-Reinhold, New York, 1979)
51. M. Heggie, B.R. Eggen, C.P. Ewels, P. Leary, S. Ali, G. Jungnickel, R. Jones, P.R. Briddon, Electrochem. Soc. Proc. **98**, 60 (1998)
52. P. Koskinen, S. Malola, H. Hakkinen, Phys. Rev. Lett. **101**, 115502 (2008)
53. D. Stull, H. Prophet, *JANAF Thermochemical Tables* (NSRDS-NBS 37, US Nat. Bur. Stand., Washington, 1971)
54. L. Girifalco, R.A. Lad, Chem. Phys. **25**, 693 (1956)
55. D. Sands, *Introduction to crystallography* (Benjamin, New York, 1969)
56. S.F. Boys, F. Bernardi, Mol. Phys. **19**, 553 (1970)
57. G. Mills, H. Jønnson, Phys. Rev. Lett. **72**, 1124 (1994)
58. G. Henkelman, B. Uberuaga, H. Jønnson, J. Chem. Phys. **113**, 9901 (2000)
59. G. Henkelman, H. Jønnson, J. Chem. Phys. **113**, 9978 (2000)
60. D. Bachellerie, M. Sizun, F. Aguillon, D. Teillet-Billy, N. Rougeau, V. Sidis, Phys. Chem. Chem. Phys. **11**, 2715 (2009)
61. Z. Šljivancanin, E. Rauls, L. Hornekaer, W. Xu, F. Besenbacher, B. Hammer, J. Chem. Phys. **131**, 084706 (2009)
62. J. Zhou, Q. Wang, Q. Sun, X. Chen, Y. Kawazoe, P. Jena, Nano Lett. **9**, 3867 (2009)
63. P.O. Lehtinen, A.S. Foster, Y. Ma, A.V. Krasheninnikov, R.M. Nieminen, Phys. Rev. Lett. **93**, 187202 (2004)
64. J. Sofo, A. Chaudhari, G. Barber, Phys. Rev. B **75**, 153401 (2007)
65. K. Xue, Z. Xu, Appl. Phys. Lett. **96**, 063103 (2010)
66. Y. Miura, H. Kasai, W.A.D. No, H. Nakanishi, T. Sugimoto, J. Phys. Soc. Jpn **72**, 995 (2003)
67. L. Chen, A.C. Cooper, G.P. Pez, H. Cheng, J. Phys. Chem. C **111**, 18995 (2007)
68. M. Bonfanti, R. Martinazzo, G.F. Tantardini, A. Ponti, J. Phys. Chem. C **111**, 5825 (2007)